efg tensor exactly coincide with the molecular coordinate system of Figure 1. In the more detailed SCCEHMO calculations they almost coincide.

The absolute values of calculated quadrupole splittings for the [II,II] and [II,III] ions are in very good agreement with the observed data (Table III). We notice that the largest efg component is still V_{yy}, i.e. the component within the pyrazine plane perpendicular to the Ru–N(bridge) direction. The sign of the efg cannot be determined from powder spectra unless the triplet structure of the two components of the spectrum is resolved or, at least, manifests itself in visible asymmetries of the pattern. Such asymmetries begin to become noticeable when the splitting Δ of the excited state exceeds about 0.5 mm s^{-1}. For [II,II] it is impossible to even guess the sign, while the [II,III] and [III,III] species are just at the limit where the sign of V_{yy} should become detectable. Owing to additional complications such as axially nonsymmetric efg tensors, unknown preferred orientation of the crystallites in the sample, and anisotropies of the Debye–Waller factor, we have to refrain from drawing any conclusions about the sign of V_{yy} from the experimental data.

The time scale of ^{99}Ru Mössbauer spectroscopy is about 10^{-8} s. For a mixed-valence compound in which the valences are trapped for times longer than about 10^{-8} s, the spectrum should show two separate doublets with different isomer shifts δ and quadrupole splittings Δ corresponding to genuine Ru(II) and Ru(III) moieties, specifically $\Delta(\mathrm{Ru(III)}) > \Delta(\mathrm{Ru(II)})$. For a mixed-valence compound with valences trapped during less than 10^{-8} s, coalescence to one doublet is expected. We interpret our experimental result as strong evidence that on the Mössbauer time scale the Creutz–Taube ion cannot be described as a localized, class II system and that there exists a strong interaction between the electronic system of the ruthenium centers and that of the pyrazine bridge.

The physical data taken together are compatible with a symmetrical structure of the two mixed-valence dimers, [II-pyz-III] and [II-bqd-III], each with two equivalent ruthenium atoms. In terms of the conventional mixed-valence language both binuclear formally Ru(II,III) ions are thus describable as delocalized or class III at least on a time scale of 10^{-8} s. In other words, if a double-well potential implying partial localization of charge is an appropriate description of [II-pyz-III] and [II-bqd-III], then it would show a central barrier of no more than 20 cm^{-1}, which is small compared to the Ru–N stretching frequencies of approximately 500 cm^{-1}.

Acknowledgment. S.J. and A.L. thank the Swiss National Science Foundation for financial support (Grant No. 2.430-0.84). The Mössbauer measurements have been funded by the German Federal Ministry for Research and Technology (BMFT) under Contract No. 03-KA1TUM-4.

Registry No. [II-pyz-II], 26253-76-9; [II-pyz-III], 35599-57-6; [III-pyz-III], 38900-60-6; [II-bqd-II], 119743-35-0; [II-bqd-III], 94890-21-8; [II-py], 21360-09-8; [II-bqd($Me)_2$], 55162-23-7; RuO_4, 20427-56-9; $Ru(NH_3)_6^{3+}$, 18943-33-4; $Ru(NH_3)_6^{2+}$, 19052-44-9; ^{99}Ru, 15411-62-8.

Supplementary Material Available: Tables SI and SII, containing Slater exponents and parameters for the charge iteration and atomic charges from SCC calculations (2 pages). Ordering information is given on any current masthead page.

Contribution from the Departments of Chemistry, McGill University, 801 Sherbrooke Street West, Montreal, Quebec, Canada H3A 2K6, and College Militaire Royal de St. Jean, St. Jean, Quebec, Canada G0G 1R0

Variable-Temperature and -Pressure Vibrational Spectra of *o*-Carborane

Ralph M. Paroli,[1a] Nancy T. Kawai,[1a] Gabriel Lord,[1b] Ian S. Butler,*[,1a] and Denis F. R. Gilson*[,1a]

Received June 3, 1988

Variable-temperature Raman and FT-IR spectra of solid *o*-carborane have been measured. Three phases (one of which is time-dependent) were detected by Raman spectroscopy, whereas four were found by using the IR technique. Variable-pressure Raman spectra up to 70 kbar revealed a phase transition at 10.1 kbar, with pressure coefficients of 1.3 and 0.75 cm^{-1}/kbar for the in-phase, B–B stretching mode of the icosahedral cage at 773 cm^{-1} in the low- and high-pressure phases, respectively.

Introduction

The icosahedral carboranes, *o*-, *m*-, and *p*-dicarba-*closo*-dodecaborane(12) ($C_2B_{10}H_{12}$) have attracted industrial attention because of their potential use in high-temperature resistant coatings and as precursors to ceramic materials such as B_4C.[2] The ortho isomer, *o*-$C_2B_{10}H_{12}$, is an orientationally disordered solid at ambient temperature and pressure, and its structural properties have been studied by X-ray diffraction,[3,4] differential scanning and adiabatic calorimetry,[3,5] and variable-temperature (300–11 K) IR,[6–8] Raman,[9–11] and ^{1}H and ^{11}B NMR spectroscopies.[12–14] While there is general agreement that an order–disorder phase transition exists for *o*-carborane at ~270 K, some authors have also reported other phase transitions occurring at lower temperatures, but these claims have been disputed.[10,11] It is clear,

o-Carborane

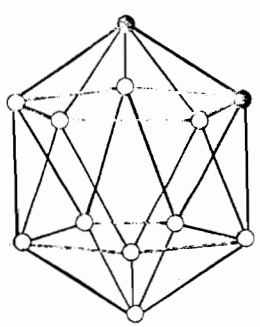

o-$C_2B_{10}H_{12}$

(1) (a) McGill University. (b) College Militaire Royal de St. Jean.
(2) Obenland, C. O.; Papetti, S. U.S. Patent 3509216, 1970.
(3) Baughmann, R. H. *J. Chem. Phys.* **1970**, *53*, 3781.
(4) Klingen, T. J.; Kindsvater, J. H. *Mol. Cryst. Liq. Cryst.* **1974**, *26*, 365.
(5) Westrum, E. F.; Henriquez, S. H. *Mol. Cryst. Liq. Cryst.* **1976**, *32*, 31.
(6) Bartet, B.; Freymann, R.; Gandolfo, D.; Mantley, F.; Rabilloud, G.; Rossarie, J.; Sillon, B. *C. R. Seances Acad. Sci.* **1974**, *279B*, 283.
(7) Selim, M.; Capderroque, G.; Freymann, R. *C. R. Seances Acad. Sci.* **1975**, *281B*, 33.
(8) Bartet, B.; Buchs, F.; Freymann, R.; Mathey, F. *C. R. Seances Acad. Sci.* **1976**, *272B*, 531.
(9) Hones, M. J.; Shaw, D. E.; Wunderlich, F. J. *Spectrosc. Lett.* **1973**, *6*, 483.
(10) Bukalov, S. S.; Leites, L. A. *Chem. Phys. Lett.* **1982**, *87*, 327.
(11) Bukalov, S. S.; Leites, L. A. *Proc. Int. Conf. Raman Spectrosc.* **1982**, *8*, 611.
(12) Leffler, A. J.; Alexander, M. N.; Sagalyn, P. L.; Walker, N. *J. Chem. Phys.* **1975**, *63*, 3971.
(13) Beckmann, P.; Leffler, A. J. *J. Chem. Phys.* **1980**, *72*, 4600.
(14) Reynhardt, E. C.; Watton, A.; Petch, H. E. *J. Magn. Reson.* **1982**, *46*, 453.

0020-1669/89/1328-1819$01.50/0

however, that the structure of this plastically crystalline material is extremely sensitive to its thermal history, regardless of the analytical technique employed.

The application of high pressure often produces the same structural changes in a sample that occur upon lowering the temperature.[15] Also, although several research groups have apparently examined the variable-temperature IR spectra of *o*-carborane, surprisingly, only spectral data for the ν(BH) region have been reported.[6-8] For these reasons, we have now investigated the phase-transition behavior of *o*-$C_2B_{10}H_{12}$: (1) under high external pressures by using a recently developed micro-Raman spectroscopic technique[16] and (2) by variable-temperature FT-IR spectroscopy.

Experimental Section

o-Carborane (Alfa Products) was purified by slow vacuum sublimation (21 °C, 10^{-3} Torr) immediately prior to use. Differential scanning calorimetric measurements were performed on a Perkin-Elmer DSC-7 calorimeter. The temperature and enthalpy calibrations were based on the phase and melting transitions of cyclohexane (Aldrich Chemical Co. Gold grade). The sample weights were typically 5–10 mg, and the samples were carefully sealed in standard aluminum DSC pans. The phase-transition temperatures and enthalpies did not show any dependence on scan rate (2.5 and 5 K min^{-1}).

The Raman and ruby fluorescence spectra were recorded on an Instruments SA U-1000 Ramanor spectrometer equipped with a Nachet optical microscope and interfaced to a Columbia Commandor microcomputer. The 514.532-nm (green) and 487.987-nm (blue) lines of a Spectra-Physics Model 164 5-W argon ion laser were used to excite the sample. The resolution employed was typically 2 cm^{-1}. A 400-μm thick gasket was mounted between the parallel surfaces of two type-IIA diamonds of a diamond-anvil cell (DAC, Diacell Products, Leicester, U.K.). The powdered ruby chip (internal pressure calibrant) and the sample were placed in the 300-μm hole of the stainless-steel gasket. Since the sample is a plastic crystal at room temperature, it was difficult to introduce into the gasket under normal conditions. This problem was surmounted by cooling the sample (with liquid nitrogen) into its ordered state, prior to placing it in the gasket. The DAC was then mounted onto an X-Y microscope stage, and a 4X microscope objective was used to focus the laser beam onto the sample. The laser powers employed were 20 mW for the sample and 10 mW for the ruby fluorescence (to avoid local heating effects). The following sequence was used when spectral measurements were made at each pressure: (1) apply pressure, (2) wait 10 min to allow the sample and ruby to reach pressure equilibrium, (3) scan the ruby fluorescence, (4) scan the Raman spectrum of the sample, and (5) rescan the ruby fluorescence region. The Raman region examined was 3000–500 cm^{-1}, but only the data for the 840–740-cm^{-1} region are reported here, since they exhibited the greatest changes.

Variable-temperature IR spectra (2-cm^{-1} resolution) were recorded between 4400 and 450 cm^{-1} on an Analect AQS-18 FT-IR spectrometer equipped with a triglycine sulfate (TGS) detector. The IR samples were examined as KBr pellets. Variable-temperature Raman studies were performed on samples sealed in glass capillary tubes, which were mounted on to the cold finger of a cryostat using indium foil as the conducting junction. All the variable-temperature vibrational data were obtained with the aid of a Cryodyne Model 21 Cryocooler (Cryogenics Technology, Inc.) and a silicon-diode temperature sensor attached to a Cryophysics Model 4025 controller (range 400–4 K). The sample temperatures remained essentially constant (±0.5 K) throughout the measurements.

Results and Discussion

Differential Scanning Calorimetry. The DSC curves revealed only one phase transition in the temperature range 330–100 K, with onset temperatures of 273.4 K on cooling and 271.0 K on heating. The enthalpy and entropy of transition were 3.25 and 12.0 J K^{-1} mol^{-1}, respectively. These results are in excellent agreement with those cited in the literature.[2,5] However, we did not observe the phase transition at 158 K reported by Westrum and Henriquez (using adiabatic calorimetry).[5] This discrepancy is most probably due to differences in sample preparation and history and possibly the scanning rate used (vide infra).

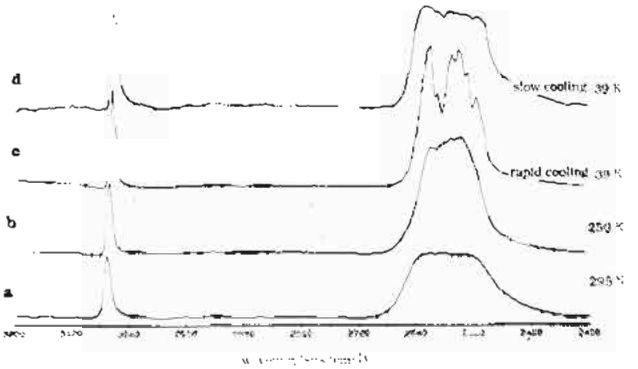

Figure 1. IR spectra of *o*-$C_2B_{10}H_{12}$ in the B–H and C–H stretching regions at (a) 295 K (phase I), (b) 250 K (phase II), (c) 39 K, following rapid cooling (phase III), and (d) 39 K, following slow cooling (phase IV).

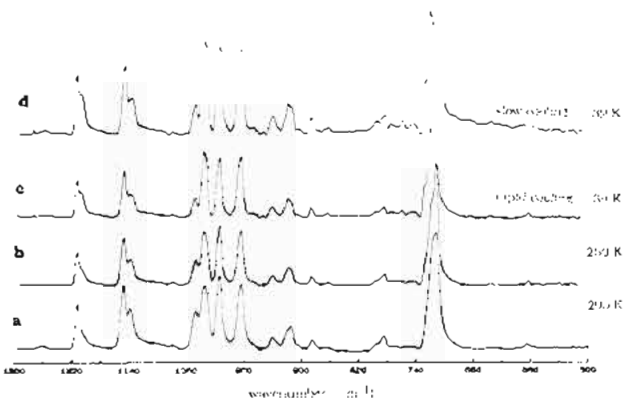

Figure 2. IR spectra of the cage vibrations of *o*-$C_2B_{10}H_{12}$ at (a) 295 K (phase I), (b) 250 K (phase II), (c) 39 K, following rapid cooling (phase III), and (d) 39 K, following slow cooling (phase IV).

Vibrational Spectra. The following scheme will be used to help in the discussion of the FT-IR and Raman spectra:

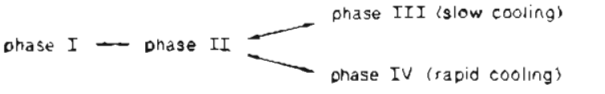

(a) Variable-Temperature FT-IR and Raman Spectra. The *o*-$C_2B_{10}H_{12}$ molecule has C_{2v} point group symmetry, and the 66 normal modes of vibration span the 21 a_1 + 13 a_2 + 16 b_1 + 16 b_2 representations. All 66 modes are Raman active. Since the a_2 modes are IR-inactive, only 53 bands should be observed in the IR spectrum. In our spectra, a total of 43 bands were detected at 295 K: 30 IR and 30 Raman bands (Table I). The missing bands may be either too weak to be observed or buried beneath stronger peaks. The proposed vibrational assignments for the observed bands are presented in Table I. The assignments are based in part on the force-field calculations for *o*- and *m*-carboranes reported by Klimova et al.[17]

The behavior of the variable-temperature IR spectra was quite peculiar (Figures 1 and 2). When the sample was cooled rapidly (about 10 K/min) from either room temperature or 250 K (i.e., from phase I or phase II, respectively) to 39 K, a new phase III resulted, which exhibited more splittings than phase II (hence ruling out the possibility of a "glassy" phase being formed). This new phase also displayed a very pronounced shoulder in the ν(CH) region, at 3061 cm^{-1}. When the sample was allowed to stand at 100 K for 3 days, the vibrational peaks became only slightly sharper. If the sample was cooled slowly from room temperature (or from 250 K) to 39 K, however, fewer splittings were observed

(15) Ferraro, J. R. *Vibrational Spectroscopy at High External Pressures: The Diamond Anvil Cell*; Academic Press, Inc.: Orlando, FL, 1984.
(16) Benham, V.; Lord, G.; Butler, I. S.; Gilson, D. F. R. *Appl. Spectrosc.* **1987**, *41*, 915.
(17) Klimova, T. P.; Gribov, L. A.; Stanko, V. I. *Opt. Spectrosc.* **1974**, *36*, 650.

Table I. Vibrational Data (cm^{-1}) for *o*-Carborane[a]

phase I (290 K)		phase II (260 K)		phase III (39 K)		
Raman	IR	Raman	IR	Raman[b]	IR	assgnts[c]
				3073 s		
3067 s	3070 s	3063 s	3064 s	3064 s	3064 s	ν(CH)
		3059 sh			3061 s	
2668 sh		2668 sh				
2632 s		2630 s				
2621 s		2623 s			2623 vs	ν(BH)
					2612 s, sh	
2609 s						
2603 s	2604 vs, br		2604 vs, br			
		2594 s			2593 vs	
		2585 s, sh			2583 vs	
2576 s		2578 s	2577 vs, br			
	2573 vs, br				2571 vs	
		2559 s			2559 s	
	1266 vw, br		1270 vw, br		1275 vw	
	1214 w		1214 w		1214 w	
1212 w		1213 w	1213 sh	1211 w		
					1209 sh	δ(HCB)
		1203 sh		1200 sh		
1150 sh	1149 w	1148 sh	1149 w	1147 vw	1149 w	b_1(1150)
	1140 vw		1139 vw		1140 vw	
1138 m		1138 w		1136 m	1138 sh	
1079 w	1080 vw, br	1080 w	1080 vw, br	1079 w	1082 vw, br	
			1051 sh		1051 sh	
1047 w	1047 w	1048 w	1047 w	1046 w	1049 vw	a_1(1050)
	1045 sh		1045 sh			
1035 w	1035 w	1037 w	1036 w	1036 w	1037 w	b_1(1040)
		1033 sh		1032 sh	1034 w	
			1015 w		1015 w	b_2(1020)
1002 w		1004 w		1003 w		
		997 w		996 w		
983 m	985 w	985 m	985 w	983 m	986 w	b_1(990)
					972 vw	
966 m	968 sh	967 m	968 sh	967 m	968 vw	δ(HBB)
		964 sh		963 sh	964 vw	
		953 vw			955 vw	
	949 vw		949 vw		949 vw	
					945 sh	
940 m	942 w	942 m	942 w	940 m	942 w	
		937 sh		937 sh		
	921 sh		921 sh		921 w	
916 s	917 s	917 s	917 w	917 s	917 sh	
	906 sh	904 vw	906 sh	903 vw	906 vw	
	886 w		887 w		888 w	
877 vw	880 sh	878 vw	880 sh	876 vw	880 vw	
862 vw	863 w	864 vw	863 w	863 vw	865 w	ν(BB),
795 s	797 w	797 s	797 w	796 s	797 vw	δ(CBB),
	789 sh		789 sh		789 sh	δ(BB)
	786 w	787 s	786 w	786 s	787 w	
					777 vw	
770 vs	768 vw	773 vw		772 vw	773 sh	a_1
		763 sh	760 vw	761 s	762 vw	
750 s	752 br, vw	752 s	750 sh	751 s	752 vw	
			744 vw	746 sh	746 vw	
		730 sh		728 sh	730 sh	skeletal
	718 sh		720 sh		724 w	
713 s	714 sh	715 s	715 m	713 s	716 s	vibrations
	638 br, vw		638 vw		638 vw	
590 m		594 m		594 m		a_2(−)
581 s	585 vw	583 s	585 vw	583 s	585 vw	
		580 s		580 s		
570 s		574 s		570 s		
562 s		566 s		560 s		
480 sh		476 w		476 w		a_2(−)
470 m		472 m		472 m		
				70 m		
				50 m		
		38 m				

[a] A fourth phase was found in the IR and Raman spectra, which differs from phase III by the presence of a peak rather than a shoulder at 3062 cm^{-1}. [b] No Raman spectral data were obtained in the ν(BH) region. [c] Values shown in parentheses are those from the force-field calculations in ref 17.

in the BH stretching region (2400–2750 cm^{-1}), and the shoulder at 3061 cm^{-1} became a well-defined peak at 3062 cm^{-1}. No spectral changes were observed for this new phase IV, even when the sample was maintained at 100 K for 3 days. It appears that, upon slow cooling (about 2 K/min), the nucleation sites of the sample may have more time to equilibrate and only one crystal

type is obtained. Upon rapid cooling, the nucleation sites do not reach equilibrium and, therefore, the formation of a metastable phase is more probable.

Some variable-temperature Raman data, using different experimental conditions, have been reported.[9-11] In the present work, the sample was cooled to 120 K and allowed to remain at that temperature. After 40 h, a new peak began to appear in the ν(CH) region at 3077 cm^{-1}, which, after 9 days, ceased to grow in intensity. The lattice region, which in phase I was featureless and in phase II showed only a single peak at 38 cm^{-1}, now contained many distinct peaks, which is indicative of a more ordered crystal. Upon slow cooling of the sample, however, the ν(CH) region did not exhibit any distinct splitting; instead, only a shoulder appeared, as was observed in the IR spectra. This same result was noted previously by Bukalov and Leites.[10,11] Note that the ν(BH) region could not be investigated under high pressure due to interference from a very strong overtone of the diamond. Clearly, kinetic effects are important, since the new peak at 3077 cm^{-1} took longer to appear at 120 K (40 h) than at 168 K (15 h). The published NMR results[3,12-14] offer some clues as to why such an effect was observed.

All the NMR results in the literature dealing with the molecular dynamics of o-$C_2B_{10}H_{12}$ indicate that the motion is isotropic in phase I but anisotropic in the low-temperature phases. The exact temperature for the transition from phase II to phase III and the nature of the motions in these phases have not been established. The reported NMR phase-transition temperatures vary from 165 to 200 K, compared with 158 K from adiabatic calorimetry. The proton line width varies smoothly with changes in temperature from 120 to 250 K. This is a wide temperature range for a motional transition and might well be a factor accounting for the difficulties in interpreting the spin–lattice relaxation-time data.

The activation energy (E_a) determined for the isotropic phase I is about 12 kJ mol^{-1}, while that for the anisotropic phases lies in the 23–40 kJ mol^{-1} range. Reynhardt and co-workers[14] suggested that the 23 kJ mol^{-1} barrier might be due to rotation about a 2-fold axis, a reasonable suggestion for the C_{2v}-symmetry icosahedral cage. On the basis of this barrier, the correlation time for molecular reorientation, τ_c, would vary from 5.9 μs at 165 K to 3 s at 120 K. The E_a values reported by Beckmann and Leffler,[13] 27 and 40 kJ mol^{-1}, were attributed to a temperature-dependent activation energy, since the high and low side of the T_1 plot produced different values. The 40 kJ mol^{-1} value leads to a τ_c of 1.3 s at 165 K and ca. 20 h at 120 K. A higher barrier would lead to an even longer τ_c value, as is suggested by our vibrational measurements.

Rapid quenching of the sample to low temperatures can freeze in disorder. The potential function governing whole molecule rotation will depend on the orientation of neighboring molecules, and therefore, a distribution of barriers will exist. This would explain the observed temperature dependence of the barriers.

(b) Variable-Pressure Raman Spectra. The effects of pressure were studied up to 70 kbar when the peaks became too broad to determine their positions with sufficient accuracy. The ν(CH) region (3100–3000 cm^{-1}) was investigated but proved to be less pressure sensitive than the 840–740-cm^{-1} region. Representative spectra in this latter range are shown in Figure 3. The 773-cm^{-1} peak has been assigned to the in-phase B–B stretching mode (a_1) of the C_{2v}-symmetry icosahedral cage.

Initially, the 773-cm^{-1} peak was relatively symmetrical, with only an extremely weak shoulder at ~765 cm^{-1}, which developed into a separate peak at a pressure of 2.9 kbar. At 5.4 kbar, the original 773-cm^{-1} peak shifted to 781 cm^{-1} and the band became sharper. As the pressure was increased to 10.1 kbar, two distinct peaks could be seen, one at 771 cm^{-1} and the other at 785 cm^{-1}. Both peaks continued to shift steadily to higher wavenumbers as the pressured was increased to 70 kbar, with the 785-cm^{-1} peak being the more pressure sensitive. The pressure dependences ($d\nu/dP$) of these two bands are shown in Figure 4.

The data indicate that there is a phase transition in o-$C_2B_{10}H_{12}$ at about 10 kbar, from its disordered face-centered cubic lattice[3,4] to a more ordered, low symmetry lattice. The pressure coefficients

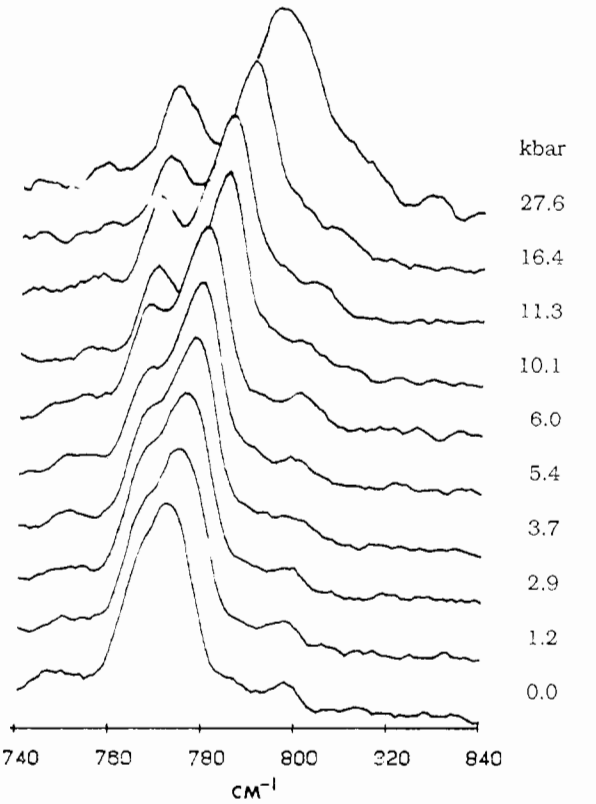

Figure 3. Variable-pressure Raman spectra of o-$C_2B_{10}H_{12}$ in the 840–740-cm^{-1} region.

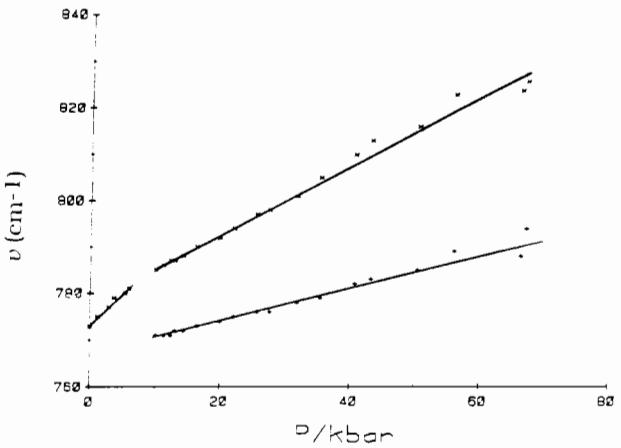

Figure 4. Pressure dependence of the 773- and 765-cm^{-1} bands of o-$C_2B_{10}H_{12}$.

for the 773-cm^{-1} peak in the two phases are 1.3 cm^{-1}/kbar (low-pressure phase) and 0.75 cm^{-1}/kbar (high-pressure phase). The pressure coefficient for the peak originating from the 765-cm^{-1} shoulder and appearing at high pressure is 0.37 cm^{-1}/kbar. These $d\nu/dP$ values are smaller than those obtained for the cesium dodecahydroborate salt, $Cs_2[B_{12}H_{12}]$ (1.6 and 1.9 cm^{-1}/kbar for the low-pressure phase and 2.1 and 2.3 cm^{-1}/kbar for the high-pressure phase)[16] but are in the same range as those for smaller caged hydrocarbons, e.g., adamantane[18] ($C_{10}H_{16}$) and adamantanone[19] ($C_{10}H_{14}O$), 0.4–1.0 cm^{-1}/kbar. The absence of a distinct discontinuity in the $d\nu/dP$ plot for o-carborane suggests that the observed phase transition is second order.

The pressure dependence of a given vibrational frequency is related to the Grüneisen parameter, γ, by eq 1, where κ is the compressibility of the molecule, ν_i^0 is the position of the vibration at ambient pressure, and P is the pressure. The compressibility

(18) Burns, G.; Dacol, F. H.; Weber, B. *Solid State Commun.* **1979**, *32*, 151.
(19) Harvey, P. D.; Butler, I. S.; Gilson, D. F. R.; Wong, P. T. T. *J. Phys. Chem.* **1986**, *90*, 4546.

$$\gamma = \frac{1}{\kappa \nu_i^0}\left[\frac{d\nu}{dP}\right] \quad (1)$$

of a molecule is therefore directly proportional to $d\nu/dP$. From our vibrational data, it appears that the low-pressure, disordered phase of o-$C_2B_{10}H_{12}$ is more compressible than the ordered, high-pressure phase.

Acknowledgment. This research was generously supported by operating and equipment grants to I.S.B. and D.F.R.G. from the NSERC (Canada) and FCAR (Quebec, Canada). The awards of graduate and postdoctoral fellowships from the same government agencies to R.M.P., N.T.K., and G.L., are also gratefully acknowledged.

Registry No. o-$C_2B_{10}H_{12}$, 16872-09-6.

Contribution from the Department of Chemistry, Princeton University, Princeton, New Jersey 08544

New Syntheses of 1,2-Ethano-*o*-carborane and the Structure of 9-Chloro-1,2-ethano-*o*-carborane†

Robert P. L'Esperance, Zhen-hong Li, Donna Van Engen, and Maitland Jones, Jr.*

Received July 12, 1988

Two new routes to 1,2-ethano-*o*-carborane (**1**) are described. Both depend on the intramolecular displacement of a leaving group by a cage carbanion. The X-ray structure of the 9-chloro derivative (**5**) was determined. Crystals of **5** are monoclinic, space group $P2_1/c$, with a = 11.456 (4) Å, b = 8.120 (2) Å, c = 12.333 (5) Å, β = 105.18 (3)°, Z = 4, and D_{calcd} = 1.23 g/cm³. The structure was solved by direct methods and refined by blocked-cascade least squares to an R value of 0.057 for 1326 independent reflections.

Introduction

Among the myriad known 1,2-disubstituted *o*-carboranes are several molecules in which the framework carbon atoms are also members of a five- or six-membered exo-cage bridge.[1] However, there is but one compound (**1**) in which the two framework carbons are members of a four-membered ring as well as the cage.[2] Our earlier synthesis of **1** was impractical, as it involved several steps, the last of which produced a number of products in comparable amounts. Accordingly, it is not surprising that no X-ray structural determination of **1** has been reported. Here we report two related new and efficient syntheses of **1** as well as the structural data on the 9-chloro derivative.

Experimental Section

General Remarks. ^{1}H NMR spectra were recorded on a General Electric QE 300 spectrometer at 300 MHz in $CDCl_3$, with signals referenced to Me_4Si. Analytical gas chromatography was performed on a Hewlett-Packard 5890A gas chromatograph with helium as carrier gas, using 2-mm-i.d. stainless steel columns packed with 3% OV 17 on Chromosorb W-HP. GC/MS runs were conducted on a Hewlett-Packard 5992B instrument, using 2-mm-i.d. glass columns packed with 3% OV 17 on Chromosorb W-HP. Preparative gas chromatography was performed on a Varian A90P gas chromatograph with helium as carrier gas. Mass spectra were obtained on a KRATOS MS 50 RFA high-resolution mass spectrometer. In general, reactions were conducted under argon. All solvents were purified and dried by using standard procedures. Melting points were determined on a Thomas-Hoover Uni-Melt or an Electrothermal Digital Melting Point Apparatus and are uncorrected.

1-(*o*-Carboranyl)-ethan-2-ol Tosylate (2). Into a 250-mL three-neck round-bottomed flask was placed 4 g (32.7 mmol) of decarborane in 50 mL of CH_3CN. The solution was refluxed under an atmosphere of argon for 2 h. The CH_3CN was removed by distillation to yield the $B_{10}H_{10}$·$2CH_3CN$ complex. This was dissolved in 50 mL of toluene and 10.5 g (46.8 mmol) of 4-tosyl-1-butyne[3] was added. The reaction mixture was refluxed under argon for 2 h. The toluene was removed by distillation to leave a gummy yellow solid. This material was placed in a Soxhlet apparatus and extracted with hexane followed by CH_2Cl_2. The organic solutions were combined, and the solvent was removed on a rotary evaporator to leave a whitish solid. This solid was purified by column chromatography on silica gel ($CHCl_3$) to give 4.5 g (40%) of a white solid, mp 112–114 °C.

^{1}H NMR ($CDCl_3$, 300 MHz): δ 7.78, 7.40 (AA'BB', 4 H), 4.11 (t, 2 H, J = 6.1 Hz), 3.69 (br s, 1 H), 2.63 (t, 2 H, J = 6.1 Hz), 2.49 (s, 3 H), 1.4–3.0 (br m, 10 H, B–H). IR (KBr): 3058, 2577, 1597, 1426, 1355, 1190, 1173, 815 cm^{-1}. Precise mass: calcd for $C_{11}H_{22}{}^{11}B_8{}^{10}B_2SO_3$ 342.2292, found 342.2246.

1,2-Ethano-*o*-carborane (1). Into a 100-mL three-neck round-bottomed flask was placed 1.5 g (4.4 mmol) of tosylate **2** in 50 mL of benzene. The flask was placed under an argon atmosphere, and 2.1 mL of 2.5 M *n*-BuLi in hexanes was added all at once. The solution was allowed to stir for 14.5 h at room temperature. The reaction mixture was poured into 25 mL of 5% HCl, and the layers were separated. The aqueous layer was extracted with 2 × 10 mL ether. The combined organic layers were washed with saturated $NaHCO_3$ solution and dried over $MgSO_4$. The solvent was removed on a rotary evaporator to leave a white solid. This material was purified by column chromatography on silica gel (hexanes) to give 0.3 g (40%) of a white waxy solid, mp 274–275 °C (sealed) (lit.[2] mp 261 °C (sealed)). Suitable crystals for X-ray analysis could not be obtained.

^{1}H NMR ($CDCl_3$, 300 MHz): δ 2.85 (s, 4 H), 1.4–3.6 (br m, 10 H, B–H).

9-Chloro-1,2-ethano-*o*-carborane (5). Into a 25-mL round-bottomed flask was placed 100 mg (0.6 mmol) of **1** and 17 mg of $AlCl_3$ in 5 mL of CCl_4. The reaction mixture was refluxed overnight. GC analysis showed the mixture to be mostly starting material. An additional 60 mg of $AlCl_3$ was added, and the mixture was refluxed for 15 min, after which time it turned dark brown. The solution was allowed to cool to room temperature and poured into 15 mL of brine. The layers were separated, the organic layer was dried over $MgSO_4$, and the solvent was removed on a rotary evaporator. GC/MS analysis showed the crude material to be a mixture of monochloro- and dichloro-substituted carboranes. The mixture was purified by preparative GC (0.25 in. × 10 ft 10% OV17 column; oven temp 160 °C), and 17 mg (14%) of a white solid, mp 192–194 °C (sealed), was obtained. Suitable crystals were obtained by slow evaporation of a heptane solution.

1-(*o*-Carboranyl)-2-bromoethane (4). A solution of 2.5 g of 1-(*o*-carboranyl)-2-hydroxyethane[4] was dissolved in 5 mL of phosphorus tribromide and stirred at room temperature for 10 h. The mixture was then dissolved in 50 mL of ether and washed with sodium bicarbonate and brine solutions. The ether was removed by rotary evaporation. The crude oil was distilled by using a Kugelrohr apparatus at 120 °C (oven)/0.1 mmHg. A yield of 2.3 g of product (69%) was obtained, mp 108–110 °C (sealed) (lit.[5] mp 114–115 °C).

^{1}NMR ($CDCl_3$, 300 MHz) δ 3.72 (s, 1 H, H–C, cage), 3.40 (t, J = 9.0 Hz, 2 H), 2.79 (t, J = 9.0 Hz, 2 H). Precise mass: calcd for

† Dedicated to Professor E. C. Taylor on the occasion of his 65th birthday.

(1) Grimes, R. N. *Carboranes*; Academic: New York, 1970. Muetterties, E. L. *Boron Hydride Chemistry*; Academic: New York, 1975.
(2) Chari, S. L.; Chiang, S.-H.; Jones, M., Jr. *J. Am. Chem. Soc.* **1982**, *104*, 3138.
(3) Brandsma, L. *Preparative Acetylenic Chemistry*; Elsevier: New York, 1971; p 159.
(4) Zakharkin, L. I.; Brattsev, V. A.; Stanko, V. I. *J. Gen. Chem. USSR (Engl. Transl.)* **1966**, *36*, 899.
(5) Fein, M. M.; Grafstein, D.; Paustian, J. E.; Bobinski, J.; Lichstein, B. M.; Mayes, N.; Schwartz, N. N.; Cohen, M. S. *Inorg. Chem.* **1963**, *2*, 1115.

0020-1669/89/1328-1823$01.50/0